Experimental Evaluation of Homogeneous Differentiators Applied to Hydraulic Stroke with Measurement Noise and Acceleration Disturbance

Benjamin Calmbach
Control Engineering Group
Technische Universität Ilmenau
Ilmenau, Germany
benjamin.calmbach@tu-ilmenau.de

Michael Ruderman
Department of Engineering Sciences
University of Agder
Kristiansand, Norway
michael.ruderman@uia.no

Johann Reger
Control Engineering Group
Technische Universität Ilmenau
Ilmenau, Germany
johann.reger@tu-ilmenau.de

***Abstract*—The design and experimental evaluation of continuous homogeneous differentiators are considered. The differentiator gains follow the high-gain setup with variable gain-scaling parameter L. This parameter results from a minimization of the effect of measurement noise and disturbance on the differentiation estimation error in terms of the homogeneous $\mathcal{L}_2$-gain. We consider and compare various homogeneity degrees including the linear (high-gain) case. It turns out that an optimum exists not only w.r.t. L but also w.r.t. homogeneity degree d. For experimental evaluation, a hydraulic cylinder controlled by a servo-valve is excited over a frequency range and the noisy cylinder stroke measurements are differentiated. Via classical metrics (root-mean-square and maximum absolute error) and a precise full-order simulation model, we evaluate the velocity estimation accuracy. Applying a second differentiation to the stroke measurements, an acceleration disturbance can be detected from a comparison of its measurement and estimate.**

I. Introduction

Differentiators come into play whenever derivatives of measurements are necessary, e.g. for control, supervision and fault detection. The differentiation of noisy signals is a demanding task since it should not unnecessarily amplify the noise level while still suppressing the effect of non-vanishing higher-order derivatives on the differentiation estimation error. There are two frameworks dominant to accomplish this task: the high-gain observer acting as a differentiator [1], [2] (i.e. linear), and the robust exact sliding-mode differentiator [3]–[5] (i.e. nonlinear, discontinuous). Both these approaches are special cases of the homogeneous differentiator [6], [7] with the respective homogeneity degrees $d = 0$ (linear) and $d = -1$ (discontinuous). Worst-case error bounds have been derived for these cases [1], [5], [8], [9], given the knowledge of the bounds on the noise and n-th order derivative of the base signal to be differentiated (n corresponds to the order of the differentiator). These lead to optimal tuning guidelines [1], [8] w.r.t. the $\mathcal{L}_\infty$-norm of the output, i.e. the differentiation estimation error. Another possibility with clear physical interpretation is the $\mathcal{L}_2$-gain to characterize the effect of measurement noise and disturbance (i.e. higher-order derivative) on the output, since it directly relates to the signal's energy. However, it turns out that the classical $\mathcal{L}_2$-gain [10] is not suitable for homogeneous systems due to its missing invariance w.r.t. homogeneous dilation [11], [12]. Hence, it is only a local property for general weighted homogeneous systems. Zhang [11] therefore introduces a generalized, global and constant *homogeneous* $\mathcal{L}_2$-gain ($\mathcal{L}_{2\mathrm{h}}$-gain) for this system class. This allows to compare the homogeneous differentiator for various homogeneity degrees, including the linear ($d = 0$) and discontinuous ($d = -1$) case. However, the $\mathcal{L}_2$-gain and $\mathcal{L}_{2\mathrm{h}}$-gain are not defined for disturbances acting on the last channel of the discontinuous differentiator. Hence, we focus on continuous, homogeneous differentiators ($d > -1$). Although a trade-off between an upper bound on the estimation error, on the one hand, and convergence time, on the other hand, has been recently proposed [8], it is out of the scope in the present evaluation. Note that, apart from $d = 0$, it is not possible to obtain the actual $\mathcal{L}_{2\mathrm{h}}$-gain yet. Still, it can be estimated [11].

Just recently, a procedure to obtain optimal differentiator gains w.r.t. the estimated $\mathcal{L}_{2\mathrm{h}}$-gain has been proposed [12], based on a Lyapunov function for the homogeneous differentiator [6], [7], and evaluated at an academic example. A practical application and evaluation is still necessary. Hence, within the present work, we adapt the approach to an experimental system and evaluate the resulting differentiator for various homogeneity degrees $-1 < d \leq 0$.

The experimental setup under consideration is a hydraulic test bench [13]–[16], as a relevant industrial application, since hydraulic cylinders are common whenever large forces and high load stiffness are demanded [17]. Mostly, it provides (noisy) stroke measurements only. Additionally, an accelerometer can be installed on the moving payload – a configuration we are also making use of for reference measurements. Often however, the cylinder velocity is necessary e.g. for fault detection, trajectories servoing and monitoring, or active vibration damping control [17]. With a detailed full-order simulation model at hand [13], the velocity-estimation error is available and allows an evaluation by means of standard metrics (root-mean-square and maximum absolute error). An application to the measurement data is in line with the simulation results.

The hydraulic cylinder controlled via servo-valve is excited over a frequency range of two decades. Besides multiple experiments with a sinusoidal excitation at distinct frequencies, a multi-sine and linear sweep are applied covering the entire frequency range. The experiments have shown an acceleration

Author´s accepted manuscript
The manuscript accepted to publication in
IEEE International Workshop on Advanced Motion Control (AMC2024)

disturbance at certain excitation frequencies that cannot be measured via relative cylinder position. However, a comparison of the cylinder acceleration estimated from the position measurements with the acceleration measurements reveals the eigenfrequency of the disturbance.

In Sec. II, we start with the problem statement to clarify the differentiator design setting. It follows a brief description of the laboratory setup (Sec. III) and the excitation signals used in experiments (Sec. IV). This covers the necessary background to proceed with the main part of the paper: design and evaluation of continuous homogeneous differentiators (Sec.V). Conclusions are drawn in Sec.VI.

Preliminaries and Notation: We use the weighted homogeneity, see e.g. [18], [19], and homogeneous input-output maps as introduced in [11]. The homogeneous norm of $x \in \mathbb{R}^n$ is defined as $\|x\|_{r_x} = \left(\sum_{i=1}^{n} |x_i|^{\frac{2}{r_i}}\right)^{\frac{1}{2}}$, where $r_x = (r_1, \ldots, r_n)$ is the positive weight vector. Further, the sign-preserving power $\lceil x \rfloor^p = \operatorname{sign}(x)|x|^p$ for $p \in \mathbb{R}$ is used.

II. Problem Statement

In the present work, we focus on a practical application of the second-order homogeneous differentiator [6], [7], [12]

$$\dot{x}_1 = -k_1 \lceil x_1 - f_\mathrm{n} \rfloor^{\frac{1}{1-d}} + x_2, \qquad x_1(0) = x_{1,0} \tag{1a}$$

$$\dot{x}_2 = -k_2 \lceil x_1 - f_\mathrm{n} \rfloor^{\frac{1+d}{1-d}}, \qquad x_2(0) = x_{2,0} \tag{1b}$$

with homogeneity degree $d \in (-1, 1)$, positive and optimized gains k_1, k_2 and states $x_1(t) \in \mathbb{R}$, $x_2(t) \in \mathbb{R}$. The (Lebesgue-measurable) noisy signal f_n can be decomposed as $f_\mathrm{n}(t) = f_0(t) - \nu(t)$ with bounded noise $\|\nu\|_\infty \leq \nu_{\max} > 0$. Given stabilizing gains (see [6], [12]) and a bounded second derivative of base signal f_0, i.e. $\|f_0^{(2)}\|_\infty \leq \delta_{\max} > 0$, the state x_2 memes the first derivative $f_0^{(1)}$ and the estimation error is ultimately uniformly bounded for $d \in (-1, 0]$ [6].

Consider the error dynamics

$$\dot{e}_1 = -k_1 \lceil e_1 + \nu \rfloor^{\frac{1}{1-d}} + e_2, \tag{2a}$$

$$\dot{e}_2 = -k_2 \lceil e_1 + \nu \rfloor^{\frac{1+d}{1-d}} + \delta, \tag{2b}$$

where $e_i = x_i - f_0^{(i-1)}$ and $\delta = -f_0^{(2)}$. They define a homogeneous input-output mapping (see [11], [12]) of homogeneity degree d w.r.t. the input $u = (\nu,\ \delta)^\top$ with weight $r_u = (1-d,\ 1+d)$, state $e = (e_1,\ e_2)^\top$ with $r_e = (1-d,\ 1)$ and output $y = e_2$ with $r_y = 1$.

If we select $d = 0$, the linear high-gain observer acting as a differentiator is recovered [1]. In contrast, for $d = -1$, we get Levant's robust exact differentiator [3]–[5].

Following the high-gain approach [1], [2], we utilize gains

$$k_1 = \alpha_1 L, \quad \text{and} \quad k_2 = \alpha_2 L^2,$$

where $\alpha_1 > 0$ and $\alpha_2 > 0$ are fixed and only $L > 0$ is a variable design parameter. This allows to proceed as proposed by [1], [12]. That means, one tries to find an optimal gain-scaling L^* that minimizes the effect of measurement noise ν and disturbance δ, which is the second time-derivative, on the differentiation estimation error $y = e_2$.

On the one hand, we minimize an estimate on the $\mathcal{L}_\infty$-gain, i.e. the maximum absolute error, for the linear high-gain differentiator ($d = 0$) using the approach of [1]. Then, we move over to the more general homogeneous case and utilize a design procedure that minimizes an estimate on the homogeneous $\mathcal{L}_2$-gain ($\mathcal{L}_{2\mathrm{h}}$-gain), – an approach recently proposed in [12]. As pointed out in detail in [11], [12], the classical $\mathcal{L}_p$-gain [10] is a local property for homogeneous systems with inputs and outputs, i.e. it is not constant w.r.t. homogeneous dilation. From this background, Zhang [11] introduces a generalized, homogeneous $\mathcal{L}_p$-gain that is also considered in this work.

Hence, the following developments focus on the design of optimal differentiator gains for various homogeneity degrees to estimate the velocity from noisy measurements. The design is evaluated via typical metrics by means of a full-order simulation model [13] and measurement data from the physical setup described below. The measurements are further utilized to estimate the frequency of an acceleration disturbance acting on the hydraulic plant.

Note that we exclude the discontinuous case $d = -1$, since the $\mathcal{L}_2$-gain (and $\mathcal{L}_{2\mathrm{h}}$-gain) is not defined for inputs acting on the last channel in this case.

For an easier presentation and adaptation to this setup in Sec. V, we follow [6], [12] and utilize the scaled error dynamics with $z_1 = e_1$, $z_2 = \frac{e_2}{L\alpha_1}$ and output $y = e_2 = L\alpha_1 z_2$:

$$\dot{z}_1 = -L\alpha_1 \left(\lceil z_1 + \nu \rfloor^{\frac{1}{1-d}} - z_2 \right), \qquad z_1(0) = z_{1,0} \tag{3a}$$

$$\dot{z}_2 = -L\frac{\alpha_2}{\alpha_1} \lceil z_1 + \nu \rfloor^{\frac{1+d}{1-d}} + \frac{\delta}{L\alpha_1}, \qquad z_2(0) = z_{2,0}. \tag{3b}$$

III. Laboratory Setup

Below described are the main parts of the hydraulic test bench, while the interested reader is refereed to [13], [14] for further details. These references also present and analyze the detailed full-order nonlinear plant model (with five states) which is used for numerical simulations in this work.

The cylinder provides an actuation range of about $0.2\,\mathrm{m}$ at frequencies up to $f_{\max} = 10\,\mathrm{Hz}$ [14]. The actuation unit is a Moog servo valve [20] with a cut-off frequency of $f_{\mathrm{c,M}} \approx 200\,\mathrm{Hz}$ and therefore sufficiently fast for this setup. It also contains a dead-zone of $\pm 10\,\%$. In the simulations as well as experiments, this is overcome by a continuous pre-compensation with $\tanh(\beta_\mathrm{p}\cdot)$, where the stiffness parameter $\beta_\mathrm{p} = 265$ is sufficiently large. This ensures that smooth excitation signals result in sufficiently smooth cylinder trajectories.

Apart from the plant actuation, the measurement instrumentation is of special interest in this article. For position measurements, i.e. the relative stroke of the cylinder, a Celesco linear-potentiometer [21] is installed. It has a sufficiently large measurement range of $0.25\,\mathrm{m}$ with analog output signal. The linearity and repeatability parameters are $0.1\,\%$ and $0.01\,\mathrm{mm}$, respectively. This device is the backbone of the present experimental evaluation. In order to detect the cylinder acceleration, a high-resolution accelerometer is utilized [22]. It provides for low noise measurements along one axis using an analog

output. With a measurement range of $\pm 2\,\mathrm{g}$, the excitation is restricted to low amplitude signals to prevent sensor saturation. Note that the position measurement is relative to the cylinder shaft, while the acceleration is measured w.r.t. the inertial system. That is, acceleration disturbances η acting on the entire test bench are not visible in the position measurements, but detectable via accelerometer as illustrated in Fig. 1.

For communication purposes with the lab computer, a real-time interface (Speedgoat baseline model S [23]) is used, where the interface cards `IO183` and `IO397` are installed. The analogue input/output channels are equipped with 16bit A/D and D/A converters and work at a sampling rate set to $f_\mathrm{s} = 2$ kHz in the conducted experiments.

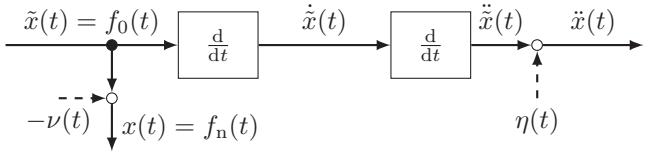

Figure 1: Schematic representation of the experimental setup.

IV. Experimental Setup and Excitation

Since the hydraulic stroke mainly acts as triple integration from valve input to cylinder position and the cylinder length is limited, the experiments are conducted in closed-loop. This ensures to keep the stroke within the actuation limits. To amplify measurement noise as little as possible, the proportional feedback gain ($k_p = 1$) is chosen sufficiently small.

The plant's reference position is in the middle of the actuator range during measurements. The excitation signals directly act on the plant, i.e. as input disturbance. For the present work, we consider multiple excitation signals within the relevant frequency range of $f_\mathrm{e} \in F = [0.1,\ 10]\,\mathrm{Hz}$. In the first scenario, 41 distinct experiments are conducted with a sinusoidal excitation for ten periods at a single frequency plus transient time. This leads to a measurement time of $T = 10 f_\mathrm{e}^{-1}$. The frequencies are logarithmically distributed over the frequency range F and the excitation amplitude is $a_\mathrm{sin} = 0.1$, such that the cylinder is prevented from saturation. As second excitation scenario, we utilize an amplitude- and band-limited multi-sine with $a_\mathrm{ms} \leq 0.25$ and $f_\mathrm{ms} \in F$ which is designed via inverse Fourier transformation and scaling of band-limited white noise. Analog to the single experiments, the measurement time is chosen to hold ten periods of the minimum frequency $f_\mathrm{low} = 0.1\,\mathrm{Hz}$, i.e. $T = 10 f_\mathrm{low}^{-1} = 100\,\mathrm{s}$. Furthermore, a linear sweep with $f_\mathrm{sweep} \in F$ is applied as third excitation scenario, where $T = 198\,\mathrm{s}$.

Exemplary measurements for a sinusoidal excitation at $f_\mathrm{sin} = 2\,\mathrm{Hz}$ are presented in Fig. 2. Both measurements (position and acceleration) are affected by noise. Still, if the setup is free of an acceleration disturbance, the position x can be reasonably estimated from the acceleration measurement $\ddot{x}$. Note that double integration yields $\bar{x}(t) = \hat{x}(t) + c_1 t^2 + c_2 t + c_3$ with constants c_1, c_2, c_3. Removing the quadratic part leads to the graph of estimate $\hat{x}$ in Fig 2a.

In case of an acceleration disturbance or sensor saturation, similar results cannot be achieved. However, the disturbance may be detected via comparison of the cylinder position's second derivative with the acceleration measurement.

Note that a full-order model of the hydraulic setup yields reliable results apart from the measurement noise, see e.g. [13]–[15]. Adding noise to the simulated position signal allows to reasonably reconstruct the measurements.

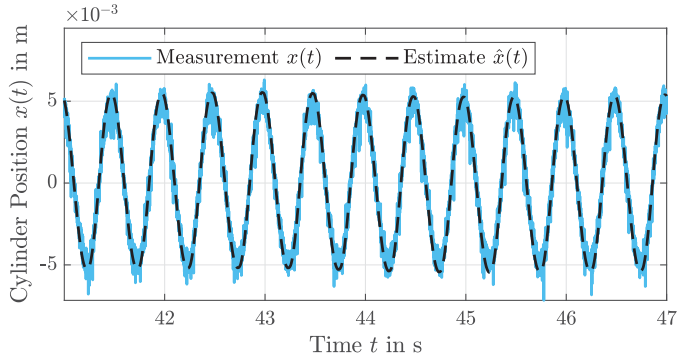

(a) Position measurement and estimation by double integration.

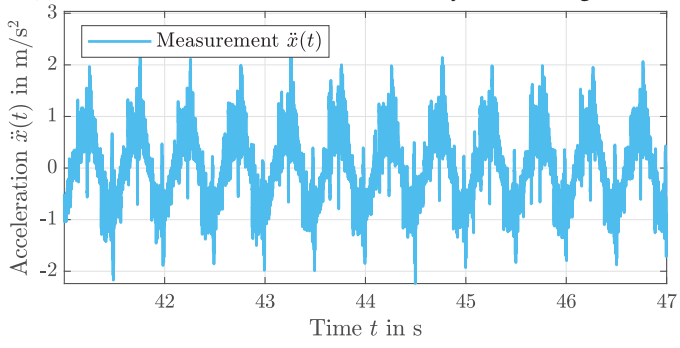

(b) Acceleration measurement.

Figure 2: Measurements of the cylinder position and acceleration during a sinusoidal excitation at $f_\mathrm{sin} = 2\,\mathrm{Hz}$.

V. Design and Evaluation of Homogeneous Differentiators

Let us design homogeneous differentiators such that the effect of measurement noise ν and disturbance δ on the differentiation estimation error $y = e_2$ is minimized. Starting from the linear case, i.e. the high-gain observer acting as a differentiator [1], the knowledge of noise and disturbance bounds is necessary. Then, Vasiljevic and Khalil [1] propose a procedure to obtain an optimal high-gain parameter ε^opt, i.e. gain-scaling $L_\mathrm{hg}^* = \frac{1}{\varepsilon^\mathrm{opt}}$, that minimizes an upper bound on the worst-case estimation error. Thus, the $\mathcal{L}_\infty$-gain is minimized. Going further to the nonlinear homogeneous case with $d \neq 0$, we utilize the bounds on noise and disturbance to scale these inputs and follow an approach to obtain optimal gain-scalings that minimize an estimate on the homogeneous $\mathcal{L}_2$-gain [12].

From steady-state measurement data we observe an upper bound on the measurement noise ν of $\nu_\mathrm{max} \approx 1.5 \times 10^{-3}\,\mathrm{m}$. For the bound δ_max on the disturbance δ, we follow a different approach. From previous works on the hydraulic system [14], an upper bound on the operation frequency $\omega_\mathrm{max} = 2\pi f_\mathrm{max}$ is

known as $f_{\max} = 10\,\text{Hz}$. The maximum measured amplitude for high-frequency sinusoidal signals is $a_{\sin} = 0.0015$. This results in $\delta_{\max} = a_{\sin}\omega_{\max}^2 \approx 6$.

A. High-Gain Differentiator

Given the bounds $\nu_{\max}$ and $\delta_{\max}$, we apply the design procedure proposed by [1]. The differentiator gains are chosen as described in Sec. II with $\alpha_1 = 2$ and $\alpha_2 = 1$ leading to multiple real eigenvalues at -1 for $L = 1$. Although conjugate-complex eigenvalues can result in smaller steady-state error, oscillatory transient response and longer transient time are possible. Thus, multiple real eigenvalues are recommended [1]. The $\mathcal{L}_\infty$-gain minimizing procedure yields (with $k = 1$, $n = 2$ and constants P_2 and Q_2 from [1])

$$\varepsilon_1^{\text{opt}} = \sqrt{\frac{0.735\nu_{\max}}{2\delta_{\max}}} = 0.009585 \quad \text{and} \quad L_{\text{hg}}^* = 104.33,$$

leading to an upper bound of $\|y\|_\infty = \|e_2\|_\infty \leq 0.23$.

B. Homogeneous Differentiator

In order to design the gains for the more general setup of homogeneity degree $d \in (-1,\ 0]$, we follow the approach proposed by [12]. This yields a (sub-) optimal gain scaling L^* which minimizes the effect of measurement noise ν and disturbance δ on the error dynamics. To apply the general results to the present case, the inputs are weighted by $\nu_{\max}$ and $\delta_{\max}$, such that the actual effect is represented. This yields the error dynamics with weighted inputs

$$\begin{aligned}\dot{z} &= f(z, \nu\,\nu_{\max}, \delta\,\delta_{\max}) \\ &= \begin{bmatrix} -L\alpha_1 \left(\lfloor z + \nu\nu_{\max} \rceil^{\frac{1}{1-d}} - z_2 \right) \\ -L\frac{\alpha_2}{\alpha_1} \lfloor z + \nu\nu_{\max} \rceil^{\frac{1+d}{1-d}} + \frac{\delta}{\alpha_1 L}\delta_{\max} \end{bmatrix}\end{aligned} \tag{4}$$

with $y = L\alpha_1 z_2$ and the homogeneous differential dissipation inequality (hDDI) [11]

$$\frac{\partial V(z)}{\partial z} f(z, \nu\,\nu_{\max}, \delta\,\delta_{\max}) + \|y\|_{r_y,2}^2 - \gamma^2 \|u\|_{r_u,2}^2 < 0,$$

where $u = (\nu,\ \delta)^\top$ with entries of comparable order. As discussed in [12], we utilize a Lyapunov function [6], [7]

$$V_1(z_1, z_2) = \frac{1-d}{2-d}|z_1|^{\frac{2-d}{1-d}} - z_1 z_2 + \frac{1+\beta}{2-d}|z_2|^{2-d} \tag{5}$$

with $\beta > 0$ for the error dynamics (3). Given an appropriate scaling a, cf. [12, Thm. 1], the function $V = aV_1$ serves as a storage function for the hDDI above and allows to estimate an upper bound $\hat{\gamma}$ on the homogeneous $\mathcal{L}_2$-gain γ. Note that the minimum value of $a = \tilde{a}L$ is independent of the inputs and, thus, Thm. 1 of [12] can be applied to the present case of weighted inputs. The hDDI results in $\hat{\mathcal{J}}(z, \nu, \delta) < 0$, where

$$\begin{aligned}\hat{\mathcal{J}}(z,\nu,\delta) = \tilde{a}\Bigg[&-\alpha_1 \left(\lceil z_1 \rfloor^{\frac{1}{1-d}} - z_2 \right) \left(\lceil z_1 + \nu\nu_{\max} \rfloor^{\frac{1}{1-d}} - z_2 \right) \\ &+ \left(-z_1 + (1+\beta) \lceil z_2 \rfloor^{1-d} \right) \left(-\frac{\alpha_2}{\alpha_1} \lceil z_1 + \nu\nu_{\max} \rfloor^{\frac{1+d}{1-d}} + \frac{\delta\delta_{\max}}{L^2\alpha_1} \right) \Bigg] \\ &+ \alpha_1^2 |z_2|^2 - \left(\frac{\hat{\gamma}}{L} \right)^2 \left(|\nu|^{\frac{2}{1-d}} + |\delta|^{\frac{2}{1+d}} \right)\end{aligned} \tag{6}$$

and its maximum w.r.t. δ can be obtained at

$$\delta^* = \left[\delta_{\max} \frac{\tilde{a}(1+d)}{2\alpha_1\gamma^2} \left(-z_1 + (1+\beta) \lceil z_2 \rfloor^{1-d} \right) \right]^{\frac{1+d}{1-d}}. \tag{7}$$

This is calculated by solving $\frac{\partial}{\partial\delta}\hat{\mathcal{J}}(z, \nu, \delta) = 0$ for δ and observing that the second derivative is negative for $\delta \neq 0$. We define $\tilde{\mathcal{J}}$ as $\hat{\mathcal{J}}$ evaluated at $\delta = \delta^*$, i.e. $\tilde{\mathcal{J}}(z, \nu; \gamma) = \hat{\mathcal{J}}(z, \nu, \delta)\big|_{\delta=\delta^*}$ and are able to calculate the $\mathcal{L}_{2\text{h}}$-gain estimate $\hat{\gamma}$ via Prop. 1 of [12]. Figure 3 illustrates the effect

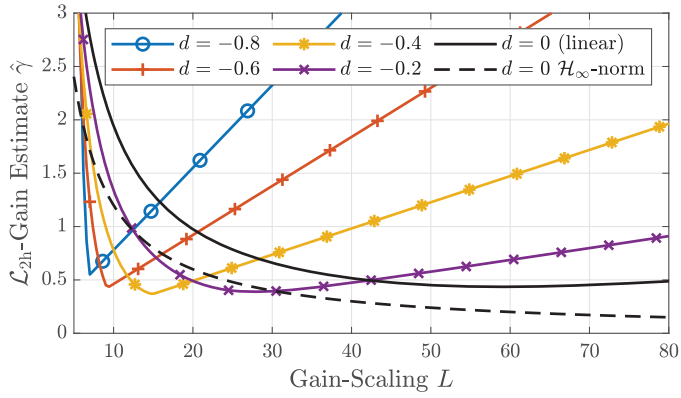

Figure 3: Homogeneous $\mathcal{L}_2$-gain estimates $\hat{\gamma}$ over gain-scaling L for homogeneity degrees $d \leq 0$.

of L on $\hat{\gamma}$ for various homogeneity degrees d. We observe the existence of an optimal scaling L^* that minimizes $\hat{\gamma}$ for each d. Apparently, the value of L^* reduces for decreasing homogeneity degrees $d < 0$. Still, the minimum $\hat{\gamma}^*$ of $\mathcal{L}_{2\text{h}}$-gain estimate $\hat{\gamma}$ remains in the same order of magnitude. In the linear case ($d = 0$), the actual $\mathcal{L}_2$-gain coincides with the $\mathcal{H}_\infty$-norm and is shown as well. Although its minimum occurs at a different value of L, the magnitude is similar to its estimate. Note that for $d \neq 0$ the actual $\mathcal{L}_{2\text{h}}$-gain cannot be calculated yet. The only consistent metric to compare various homogeneity degrees is, therefore, its estimate $\hat{\gamma}$.

According to Fig. 3 and [12, Thm. 2], a minimization of the $\mathcal{L}_{2\text{h}}$-gain estimate w.r.t. gain-scaling L is possible. For this purpose, we utilize a bisection algorithm and obtain the respective optimum values of $\hat{\gamma}^*$ and L^* in Fig. 4. We observe a minimum estimate of $\hat{\gamma}^* = 0.37$ at $d \approx -0.4$ with $L^* = 14.95$. Note that the previously designed high-gain scaling L_{hg}^* leads to the significantly higher estimate $\hat{\gamma}_{\text{hg}}$

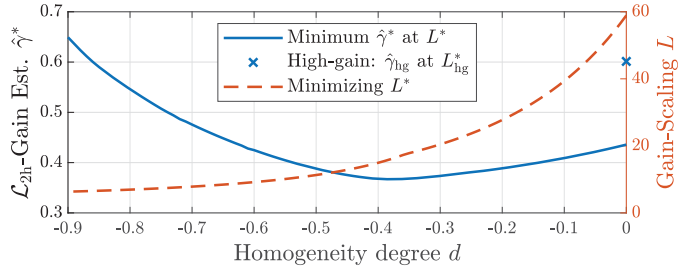

Figure 4: Minimizing gain-scaling L^* and respective $\mathcal{L}_{2\text{h}}$-gain estimates $\hat{\gamma}^*$ for various homogeneity degrees $d \leq 0$ and for the high-gain case of Sec. V-A.

also shown in Fig. 4. Having obtained minimizing gain-scalings L^* for various homogeneity degrees, we evaluate the differentiators at the hydraulic system to estimate the velocity from noisy position measurements.

C. Evaluation

For comparison of the differentiators, we utilize the full-order simulation model provided by [13] within Matlab/Simulink® and a fixed-step solver ($\tau = 0.0005\,\mathrm{s}$). Band-limited white noise with appropriate power (i.e. fitting to the measurements) is added to the cylinder output position. Thus, noise-free velocity data from simulation can be compared to the differentiated noisy position data. The evaluation metrics are chosen as maximum absolute error and root-mean-square (RMS) error defined as

$$y_{\max} = \max_{i=1,\dots,N} |y_i| \quad \text{and} \quad y_{\mathrm{RMS}} = \left(\frac{1}{N} \sum_{i=1}^{N} y_i^2 \right)^{\frac{1}{2}},$$

where N is the number of measurements and $y_i = y(i\tau)$. Note that these are of special interest, since the RMS error coincides with a normalized two-norm, whereas the maximum absolute error directly relates to the infinity-norm.

The excitation signals described in Sec. IV are applied to the full-order model and lead to the noisy position data. We compare differentiators with various homogeneity degrees, where the linear case ($d = 0$) is further compared to the optimal high-gain scaling L^*_{hg}. The results for sinusoidal excitation at distinct frequencies $f_{\sin} = 0.1, \dots, 10\,\mathrm{Hz}$ are summarized in Fig. 5. As expected for the linear case (black) the error metrics are frequency-dependent, i.e. better performance is achieved for smaller frequencies. Furthermore, the $\mathcal{L}_\infty$-optimal tuning yields better high-frequency results due to its higher value of L^*. Given the present choice of gain-scalings, the benefit of a nonzero homogeneity degree $d < 0$ is visible for higher frequencies only. The band-limited noise yields more distributed maximum error metric. Still, similar conclusions can be drawn.

Table I: Minimizing gain-scalings L^* and resulting RMS $y_{\mathrm{RMS},i}$ and maximum absolute error $y_{\max,i}$ metrics for the multi-sine ($i = 1$) and linear sweep ($i = 2$) excitation signals.

d	**0** (HG)	**0**	**−0.2**	**−0.4**	**−0.6**	**−0.8**
L^*	104.33	58.91	27.72	14.95	9.27	7.13
$y_{\mathrm{RMS},1}$	0.019	0.024	0.020	0.018	0.019	0.024
$y_{\max,1}$	0.088	0.102	0.092	0.085	0.086	0.110
$y_{\mathrm{RMS},2}$	0.020	0.026	0.021	0.019	0.020	0.024
$y_{\max,2}$	0.084	0.087	0.084	0.086	0.090	0.116

The results for the remaining excitation signals are summarized in Table I. As expected from Fig. 4, the best RMS error metric is achieved with homogeneity degree $d = -0.4$. Still, the $\mathcal{L}_\infty$-optimal scaling (HG) yields comparable results and indicates that the $\mathcal{L}_{2\mathrm{h}}$-optimal approach is highly dependent on the chosen storage function V leading to $\hat{\gamma}^*$ at L^* as pointed out by [11], [12]. Apparently the homogeneity degree plays only a minor role for the presented metrics of Tab. I, given the optimal gain-scaling L^* for each case.

Having compared the differentiators by means of the full-order simulation model and knowing the model precision [13], [14], these results can be extended easily to the measurement data. To recapitulate an exemplary experiment of Sec. IV, we pick a homogeneous differentiator with $d = -0.4$ and $L^* = 14.95$ to differentiate the position measurement. As a comparison, the acceleration measurements are integrated once and the linear drift is removed. The results are shown in Fig. 6 and fit the previous observations.

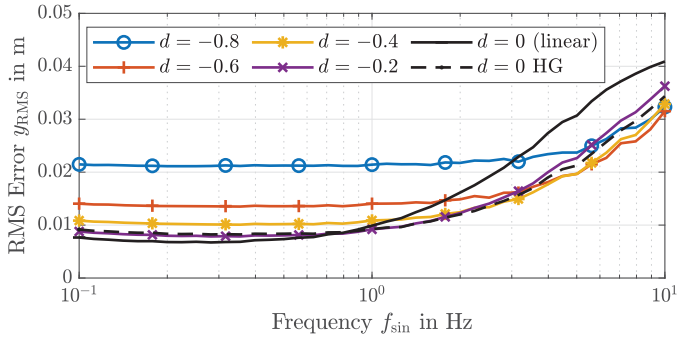

(a) RMS error values y_{RMS}.

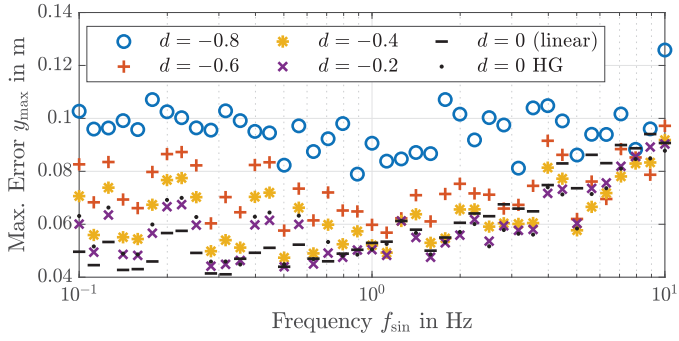

(b) Maximum absolute error $y_{\max}$.

Figure 5: Differentiation estimation error metrics for sinusoidal excitation with $f \in F$ for various homogeneity degrees d, including the linear case ($d = 0$) and high-gain differentiator (HG). The gain-scalings L^* correspond to Tab. I.

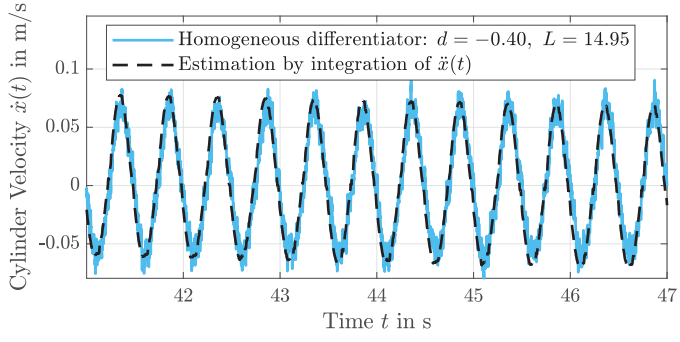

Figure 6: Velocity estimation from noisy data by applying the homogeneous differentiator to the position measurement and integrating the acceleration data of Fig. 2, respectively.

D. Acceleration Disturbance

On top of the previous results, we consider the detection of an acceleration disturbance. As discussed in Sec. III, the accelerometer detects acceleration w.r.t. the inertial system,

while the linear potentiometer measures the relative cylinder position. Thus, if an acceleration disturbance acts on the plant, it remains invisible only in the measured position.

When the plant is excited by the linear sweep described in Sec. IV, parasitic oscillations of the test setup can be observed. These are aimed to be detected in the following. For that purpose, we apply the differentiator with $d = -0.4$, according to Tab. I, twice to the position measurements and compare the frequency spectra of the acceleration measurement $\ddot{x}$ with the twice differentiated position signal as depicted in Fig. 7. The plant input with constant frequency spectrum is shown

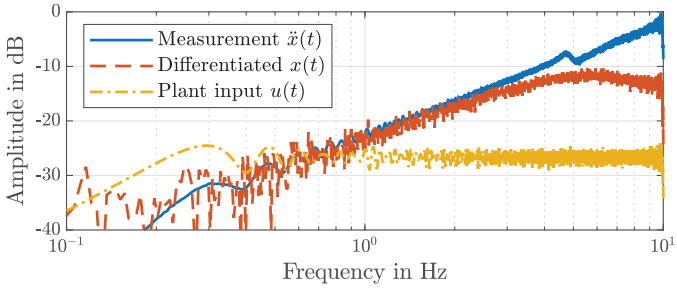

Figure 7: Frequency spectra of the cylinder acceleration measurement and estimation by differentiation of the position measurement for a linear sweep excitation.

as well. Since the poles of the nominal model [15] are two orders of magnitude faster than the excitation frequency range, we do not expect peaks in the presented frequency spectrum. This coincides with the double differentiation of the relative cylinder position signal x. Hence, the peak of the acceleration measurements $\ddot{x}$ coincides with the frequency $f_p \approx 4.75\,\mathrm{Hz}$ of the parasitic oscillations, i.e. the test bench's eigenfrequency. This allows detection of parasitic oscillations, while over lower frequency range the spectra of the measurement and double differentiation are inline with each other.

VI. Conclusions

Designing continuous homogeneous differentiators of various degrees $d \in (-1, 0]$ for the present setup is based on the minimization of the homogeneous $\mathcal{L}_2$-gain from measurement noise and disturbance on the differentiation estimation error. With the bounds on noise and disturbance from the measurement data, a recent approach is adapted to the present hydraulic system. It turns out that not only a minimum of the estimated $\mathcal{L}_{2\mathrm{h}}$-gain exists with respect to the gain-scaling L, also a minimizing homogeneity degree of $d \approx -0.4$ can be observed. The differentiation of noisy position measurements yields reasonable results for excitation signals in a relatively broad frequency range of two decades, and is in accord with the expectations. A further application of the differentiator allows to detect the frequency of an acceleration disturbance in the system structure.

References

[1] L. K. Vasiljevic and H. K. Khalil, "Error bounds in differentiation of noisy signals by high-gain observers," *Sys. & Contr. Lett.*, vol. 57, no. 10, pp. 856–862, 2008.

[2] H. K. Khalil, *Nonlinear systems*. Prentice Hall, 2002.

[3] A. Levant, "Robust exact differentiation via sliding mode technique," *Automatica*, vol. 34, no. 3, pp. 379–384, 1998.

[4] A. Levant, "Higher order sliding modes and arbitrary-order exact robust differentiation," in *European Control Conference*, 2001, pp. 996–1001.

[5] A. Levant, "Higher-order sliding modes, differentiation and output-feedback control," *International Journal of Control*, vol. 76, no. 9-10, pp. 924–941, 2003.

[6] E. Cruz-Zavala and J. A. Moreno, "Lyapunov functions for continuous and discontinuous differentiators," in *IFAC NOLCOS*, 2016, pp. 660–665.

[7] E. Cruz-Zavala and J. A. Moreno, "Levant's arbitrary-order exact differentiator: A lyapunov approach," *IEEE Trans. Aut. Cont.*, vol. 64, no. 7, pp. 3034–3039, 2019.

[8] R. Seeber, "Worst-case error bounds for the super-twisting differentiator in presence of measurement noise," *Automatica*, vol. 152, p. 110 983, 2023.

[9] R. Seeber and H. Haimovich, "Optimal robust exact differentiation via linear adaptive techniques," *Automatica*, vol. 148, p. 110 725, 2023.

[10] A. van der Schaft, *L2-Gain and Passivity Techniques in Nonlinear Control*. Springer, 2017.

[11] D. Zhang, J. A. Moreno, and J. Reger, "Homogeneous $\mathcal{L}_p$ stability for homogeneous systems," *IEEE Access*, vol. 10, pp. 81 654–81 683, 2022.

[12] B. Voß, J. A. Moreno, and J. Reger, "Minimizing the Homogeneous $\mathcal{L}_2$-Gain of Homogeneous Differentiators," preprint at arXiv: 2311.10519 [eess.SY].

[13] M. Ruderman, "Full- and reduced-order model of hydraulic cylinder for motion control," in *IEEE IECON*, 2017, pp. 7275–7280.

[14] P. Pasolli and M. Ruderman, "Linearized piecewise affine in control and states hydraulic system: Modeling and identification," in *IEEE IECON*, 2018, pp. 4537–4544.

[15] R. Checchin, M. Ruderman, and R. Oboe, "Robust two-degrees-of-freedom control of hydraulic drive with remote wireless operation," in *IEEE Int. Conf. on Mechatronics*, 2023, pp. 1–6.

[16] M. A. Estrada, M. Ruderman, and L. Fridman, "Super-twisting based sliding mode control of hydraulic actuator without velocity state," *Control Engineering Practice*, vol. 142, p. 105 739, 2024.

[17] M. Jelali and A. Kroll, *Hydraulic Servo-systems: Modelling, Identification and Control*. Springer, 2003.

[18] S. P. Bhat and D. S. Bernstein, "Geometric homogeneity with applications to finite-time stability," *Math. of Contr., Sign., Sys.*, vol. 17, no. 2, pp. 101–127, 2005.

[19] A. Bacciotti and L. Rosier, *Liapunov Functions and Stability in Control Theory*. Springer, 2005.

[20] MOOG, *Datasheet D633 R16KD1M0NSM2*, 2020.

[21] Celesco, *Datasheet CLP-250*, 2017.

[22] Micromega, *Datasheet iac-hires-ud-01*, 2021.

[23] Speedgoat, *Baseline real-time target machine*, 2022.